sustainability

MDPI

Article

Channel Evolution under the Control of Base-Level Cycle Change and the Influence on the Sustainable Development of the Remaining Oil—A Case in Jiang Ling Depression, Jiang Han Basin, China

Wei Zhu [1,2], Mingsu Shen [1], Shixin Dai [1,2,*], Kuanning Liu [3] and Yongdi Qi [1]

[1] School of Earth Sciences and Spatial Information Engineering, Hunan University of Science and Technology, Xiangtan 411201, China
[2] Hunan Key Laboratory of Shale Gas Resource Utilization, Hunan University of Science and Technology, Xiangtan 411201, China
[3] Faculty of Cultural Communication and Art Design, Hunan College of Information, Changsha 410200, China
* Correspondence: 8530003@hnust.edu.cn

Abstract: The extension of river channels is one of the key factors in determining the remaining oil distribution. Different sedimentary facies and bedding types of oil layers will form specific characteristics of remaining oil distribution after water injection development. Using massive drilling, core, logging, seismic, and production data, on the basis of sequence stratigraphy base-level cycle change, the river records and development history are restored, and the fine connectivity of reservoirs and the configuration relationship of production wells are studied. The following conclusions are drawn: (1) A sequence stratigraphic division scheme is established. In the established sequence framework, the types and characteristics of reservoir sand bodies are analyzed. The 2nd and 6th members of Yu yang formation can be divided into 2 long-term base level cycles, 5 medium-term base level cycles, and 17 short-term base level cycles. The evolution of the second and sixth members of the Yu yang formation shows a pattern of base level rising, falling and rising again; (2) the vertical sedimentary evolution sequence is underwater distributary channel distributary channel meandering channel distributary channel flood plain. The types of channel sand bodies developed from little overlap to more vertical or lateral overlap and then gradually changed to isolated type; (3) according to the structural location and development sequence, different types of reservoirs are identified. Combined with the statistics of the drilled data of Yu yang formation k_2y4 in Fu I fault block, it is found that the connectivity rate of oil layer thickness (the ratio of oil layer connectivity thickness to total thickness of sand layer) within the oil-bearing area is 84.4%, and the connectivity rate of the number of layers (8) is 60%. The connectivity condition is relatively good.

Keywords: high-resolution stratigraphic sequence; base level cycle change; sedimentary microfacies; sand body development; remaining oil distribution

Citation: Zhu, W.; Shen, M.; Dai, S.; Liu, K.; Qi, Y. Channel Evolution under the Control of Base-Level Cycle Change and the Influence on the Sustainable Development of the Remaining Oil—A Case in Jiang Ling Depression, Jiang Han Basin, China. *Sustainability* **2022**, *14*, 12518. https://doi.org/10.3390/su141912518

Academic Editors: Jianbo Tang, Wentao Yang and Xuexi Yang

Received: 12 August 2022
Accepted: 28 September 2022
Published: 30 September 2022

1. Introduction

The oil and gas exploration in the Jiang ling Depression of the Jiang han Basin is facing a severe situation where the exploration degree and proven degree are increasing, and the proportion of concealed and low-permeability oil and gas reservoirs is increasing, while the reserve size and effective total reserves of unit reservoirs are decreasing, and further exploration is extremely difficult. Although the area's exploration degree and proven degree are high, the remaining resources and average remaining oil and gas resources are 37.61 million tons and 26.58 million tons, respectively, and there is still a large exploration potential to be explored.

The Jiangling depression has been comprehensively studied in terms of geotectonic transport and hydrocarbon formation, especially in terms of the various tectonic evolution-

ary stages [1–13]. During the study of the formation of the Wan cheng Fracture Zone in the depressional tectonic evolution, it was found that the main faults in the Wan cheng Fracture Zone were active from the end of the Cretaceous and tended to end during the deposition of the Jing Sha Formation. In terms of reservoir formation, the reservoir genesis and reservoir types were described in the region, i.e., the Wan cheng Fracture Zone formed better trap conditions during the fault-pass stage of the Sha shi Formation.

The extensibility of the river is one of the key factors in determining the remaining oil distribution [14–21]. The different sedimentary facies of oil reservoirs as well as the type of stratigraphy, etc., will form specific characteristics of the remaining oil distribution after water injection and development. The reservoir non-homogeneity of terrestrial reservoirs is strong, and the distribution pattern of remaining oil in sandstone is complex, so the accurate analysis of reservoir sand structure to control the remaining oil becomes the main goal of field development and adjustment [22–31]. The distribution pattern of the main reservoir sand types in the onshore oil and gas-bearing basin of Jiangling Depression in Jiang han Basin is as follows: alluvial-flat plain sand bodies are mainly developed in the western high fault stage of Xie Feng qiao fault; curvilinear river–deltaic sedimentary sand bodies are developed in the Fu Xing chang fault block; and submerged divergent river sand bodies are mainly developed in the area west of Xie Feng qiao. By establishing a more precise isochronous stratigraphic and sedimentary micro-facies framework, the remaining oil distribution can be analyzed more effectively. [32–45] The identification of the type of stratigraphic structure and superposition pattern controlled by the basement gyre and its position in the advanced gyre in the terrestrial river–lake environment has become a key issue in the study of the remaining oil distribution in terrestrial basins [46–61].

In this study, the relationship between the remaining oil distribution and geological structure is analyzed and compared based on drilling, core, logging, seismic, and production data based on changes in the base-level cycles in sequence stratigraphy; additionally, the comparative analysis of reservoir fine connectivity and the configuration relationship of producing wells is studied, taking the Jiang han Basin Jiangling Depression Fu I fault block as an example. Guidance is provided for the sustainable recovery of the remaining oil.

2. Geological Setting

The Jiang ling Depression, located in Song zi City in the southern part of the Jiang han Basin, is the largest secondary tectonic unit in the Jiang han Basin and the second most hydrocarbon-rich depression after the Qian jiang Depression. The Jiang ling Depression is based on the metamorphic rocks from the Upper Sword to the Upper Paleozoic and the sedimentary rocks of the Sinian to Jurassic systems. The maximum thickness of the Middle Cenozoic strata deposition is nearly 9000 m, and the Cretaceous, Paleoproterozoic, and Neocene strata are well developed. The structural pattern of Jiang ling Depression has the characteristics of an east-west block and a north-south belt. It was bounded by the Wan cheng fault belt and the Jiang kou syncline belt in the west, also known as the Jiang kou depression. From north to south, the east is divided into five structural units: the Shi qiao monoclinal belt, Qing shui kou syncline belt, Jing zhou anticline belt, Zi fushi syncline belt, and Gong monocline belt, which are collectively known as the Jiang ling Depression (Figure 1a,b).

A series of breakthroughs in oil and gas exploration from the Paleogene Xin gou zui Formation and Sha shi Formation to the Cretaceous Yu yang Formation on the Wan cheng–Xie Feng qiao fault belt in the southwest of the Jiang ling Depression provide detailed evidence for the oil control of the structural slope break belt of the continental faulted lake basin.

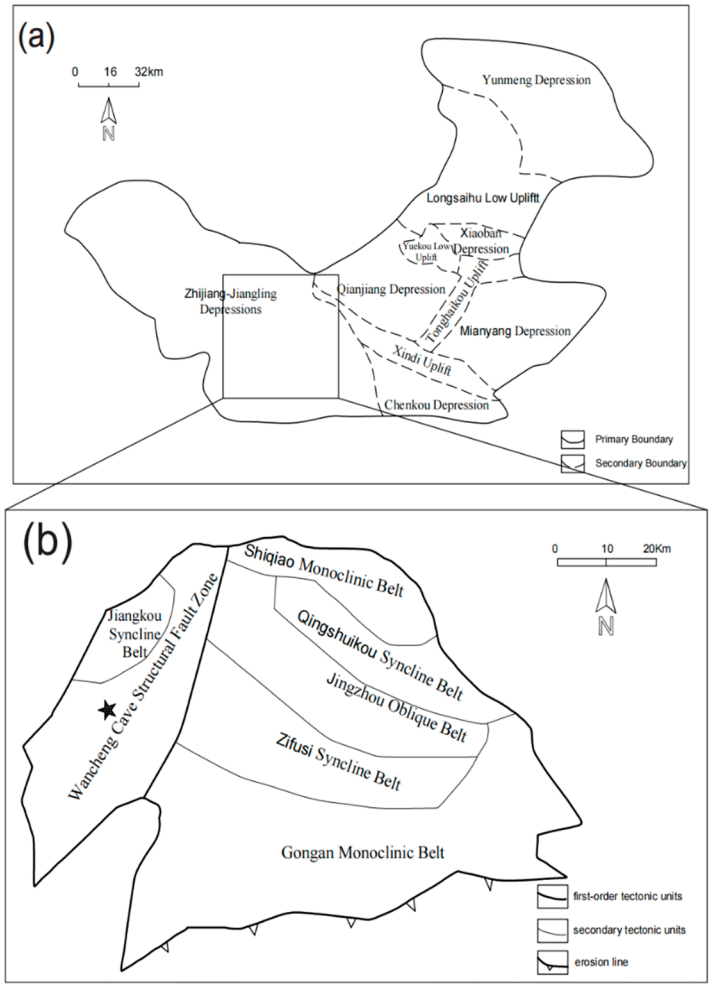

Figure 1. (**a**) Location of Jiang han Basin and the research area (**b**) Regional geological map of the study area.

3. Materials and Methods

3.1. Sedimentary Facies Method

Previous research has shown that the western part of the Jiang ling Depression in the Jiang han Basin was a fault basin during the Cretaceous-Paleocene Sha Shi Formation deposition, when the terrain was relatively flat and gentle and the climate was arid. The gentle slope drop, paroxysmal flooding events, and short distance transport of multiple sources result in periodic flooding sedimentation in this area. With the intensification of tectonic fracture activity, the topographic difference becomes larger, and the slope becomes steeper, gradually developing high curvature curvilinear river deposition. Then, in the deltaic plain, a number of branch rivers flow into the lake. The river-controlled delta is developing. The curvilinear river-flood plain sedimentation combination (Figure 2) developed over a long time in the complex fault block, and its vertical and planar sedimentary facies characteristics are analyzed below.

3.1.1. Analysis of Core Sedimentary Microfacies of Yu Yang Formation in Typical Well SK10

Well SK10 is located in the Fu I fault block. It is a well with a relatively complete stratigraphic sequence, so we take it as a standard well. The mudstone in the upper member of the Yu yang formation encountered in this well is mainly brown, followed by red-brown and brown-gray. The sandstone is mainly light gray, dark gray, and brown-gray with relatively coarse particle size, mainly coarse silt and fine sand. According to the analysis of core and thin section data, the sandstone has good sorting performance, and the roundness

is mostly sub-round or sub-angular. The texture is relatively pure. The clastic composition is mainly quartz, accounting for 70–86%, followed by feldspar, accounting for 6–15%, with a small amount of dark minerals. At the same time, cement content accounts for 15–25%. According to statistics, the thickness of a single layer of sandstone is generally 1–2.5 m, the thickest is about 11 m, and the total thickness is 138.3 m, 38.5% of the total thickness of the occupied layer. On the contrary, chemical rocks (gypsum mudstone and salt rock) are not developed in this section, reflecting that the sedimentary water body is fresh water.

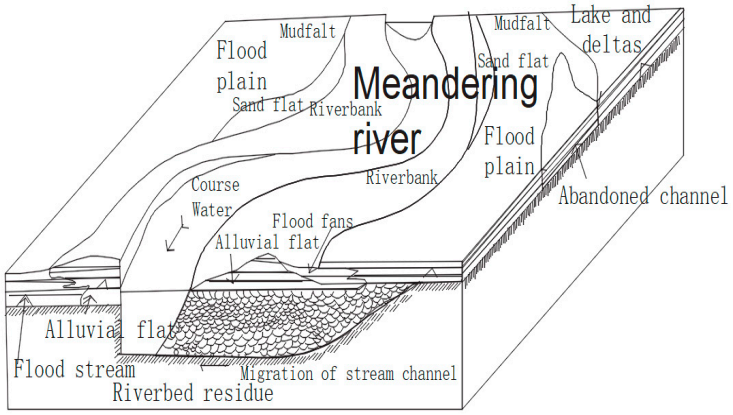

Figure 2. Sedimentary model map of Cretaceous flood plain—meandering river in Jiang ling Depression.

According to the core observation, the horizontal bedding, biological burrows, and biological disturbance structures are developed in the red-brown mudstone. The sorting of light gray sandstone is poor, with parallel bedding, oblique bedding, trough and plate cross bedding, traction and collapse structures, and the scouring surface and mud gravel are developed at the bottom of the sandstone, which belongs to the residual deposition of the riverbed. The sandstone is in abrupt contact with the underlying mudstone. The lithology combination is from bottom to top, and the particle size is from coarse to fine. The upper part is dominated by mudstone, and the lower part is dominated by sandstone. It has typical fluvial facies binary structure characteristics. The electrical logging curve has obvious multi-stage positive cycle rhythm characteristics, which is generally the sedimentary environment of flood lake meandering fluvial facies.

In addition, according to the characteristics of the normal probability distribution curve of channel facies particle size of the Yu yang formation in well KS10 (Figure 3), the particles are composed of both jumping and suspended populations, the former accounting for about 65% and the latter for about 35%. The truncated inflection between the two is clear, and there is no nudging total, indicating that the environment of channel sand body in this area is neither a braided river near the foothills nor a distributary river in the delta plain. It is a meandering river with medium and low curvature flowing from the northwest to the southeast.

3.1.2. Analysis of Well SK10 Logging Curve

The microfacies of well SK10 at the 3368.96–3377.79 m well depth section are composed of point bar-mudflat-sandflat-mudflat-flood plain from top to bottom. The top part is brownish-gray fine sandstone that belongs to the point bar microfacies. The middle part is interbedded with gray argillaceous siltstone and brownish-red mudstone layers that belong to the mudflat and sandflat microfacies. The lower part is interbedded with muddy siltstone and silty mudstone layers that belong to the flood plain microfacies (Figure 4).

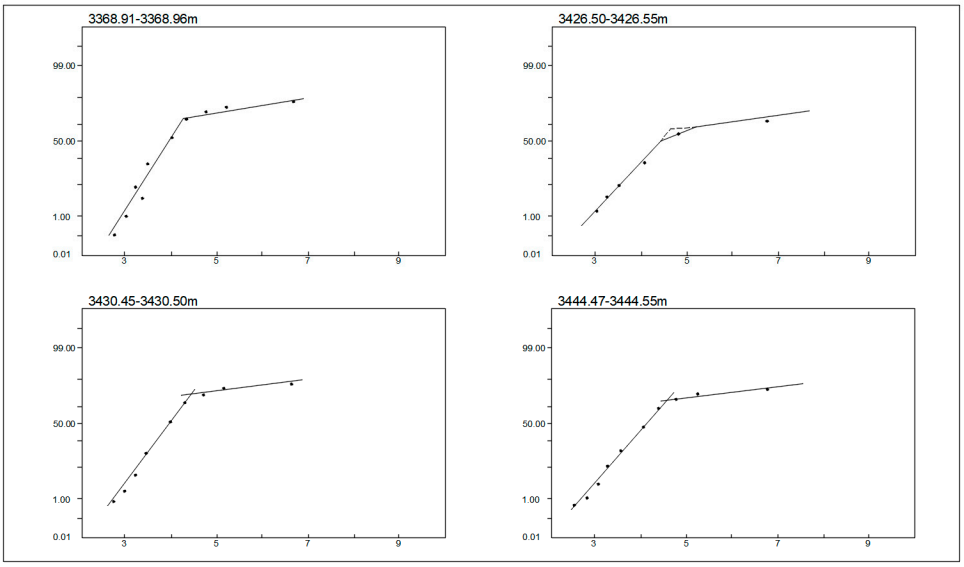

Figure 3. Probabilistic curve of river facies granularity of Yu yang Formation in Well SK 10.

Figure 4. Sedimentary microfacies characteristics of core logging curve in 3368.96–3377.79 m well depth section.

The microfacies of well SK10, 3422.35–3430.50 m well depth section, are composed of a meandering channel-floodplain and a natural barrier meandering channel from bottom to top. The bottom of the gray sandstone microfacies in the lower part has an undercut scouring surface and is filled with mud gravel. The particle size becomes finer upward. The spontaneous potential curve is bell-shaped, which is a typical positive rhythm. The middle part is brownish gray and varies from silty mudstone to argillaceous siltstone, belonging to the flood plain microfacies. The upper part is a meandering channel (Figure 5).

3.1.3. Type of Sedimentary Microfacies

Based on the study of regional sedimentary facies, combined with the shape of the logging curve and vertical lithology combination, it can be seen that the sedimentary strata of the Cretaceous Yu yang formation in Fu I fault block are mainly the combination mode of the flood plain, meandering river sedimentary facies, distributary channel, and delta underwater distributary channel. Meandering rivers include meandering channels, floodplains, natural dike, and crevasse fan microfacies; flood plains include sandflats, mudflats, and other microfacies; and microfacies of distributary channels and underwater distributary channels at the place where the river enters the lake.

According to the characteristics of the sedimentary microfacies profile, sand isogram, logging curve characteristics, and planar contact relationship, the planar distribution of sedimentary microfacies was drawn. After the analysis of core and logging curves, the sedimentary facies of K_2y1-K_2y4 of the Yu Yang Formation in the Fu I fault block is mainly river deltaic facies, and the reservoir is channel deposits.

Figure 5. Sedimentary microfacies characteristics of core logging curve in 3422.35–3430.50 m well depth section.

3.2. Identification Mark Method of Base Level Cycle Interface

The Yu yang Formation in the Yuan shi area is a complete basal falling–rising cycle combination, with a set of thick sandstones as the top boundary at the bottom of the overlying Sha shi and a large set of mudstones in the underlying Yu yang Formation, which is more stable in regional distribution and is a lake-flood surface deposit in the Jiang ling Depression that can be used as a tertiary sequence comparison marker (Figure 6a,b). The top interface of the mudstone is at the inflection point where the natural gamma value decreases abruptly upward, and the seismic profile is an obvious reflection layer of the T10 wave group with strong amplitude, low frequency, and good continuity, which is a stable set of reflection axis in the region, can be continuously traced for comparison, and is a stable layer as a regional time stratigraphic comparison marker (Figure 6c).

Research manuscripts reporting large datasets that are deposited in a publicly available database should specify where the data have been deposited and provide the relevant accession numbers. If the accession numbers have not yet been obtained at the time of submission, please state that they will be provided during review. They must be provided prior to publication.

3.2.1. Lithological Changes and Facies Signs

The cycle of development and transformation of river sand body can be inferred from sediment color, sedimentary structure, sand mudstone thickness, and bottom scouring surface. ① Because the bottom scouring structure may have different bottom scouring surfaces caused by channel undercutting and filling under different hydrodynamic conditions in different periods, the genetic type of reservoir sand body can be inferred (Figure 6a). ② Sedimentary discontinuities, such as brownish-red mudstone developed at 3377.79 m from the coring of well SK10, are generally easy to form in the nearshore belt, and the sediments are obviously differentiated, mostly containing calcareous mudstone and plant rhizome fossils, which can be used as the short-term cycle interface within the Yu yang formation (Figure 6b). ③ Lithologic lithofacies conversion interface. For example, the positive rhythmic facies sequence reflects the upward shallowing sedimentary process, and the anti-rhythmic facies sequence reflects the upward deepening sedimentary process. The conversion of the two can be used as the sequence division interface. The sedimentary con-

version surface is mainly the internal interface of the Yu yang formation, and the slope belt is mostly the bottom interface of the channel retrograde superposition style sand body. In the part where mudstone is widely developed in the lower part of the slope belt, it is mostly a set of thin sheet sand or conversion surface inside argillaceous rock, and its resistivity is high. The para-sequence model is characterized by the development of channel retained sediments and laterally accreted channel sand bodies at the bottom of a meandering river, and then shallowing upward, and the development of mudstone deposits in the flood plain. On the seismic profile, the phenomenon of upwarping can be seen locally, and the unconformity sequence boundary can be limited to the third-order sequence or long-term cycle boundary. ④ Where the thickness of sand and mudstone changes obviously, for example, from bottom to top, the content ratio of sand and mudstone decreases upward, and the particle size becomes finer upward, showing the characteristics of positive cycle change. ⑤ The color of mudstone can be used as a sign of facies. For example, grayish-green mudstone in shallow water delta facies indicates the underwater reduction environment of the delta front, and brownish red mudstone indicates the onshore oxidation environment of the delta plain (Figure 6a).

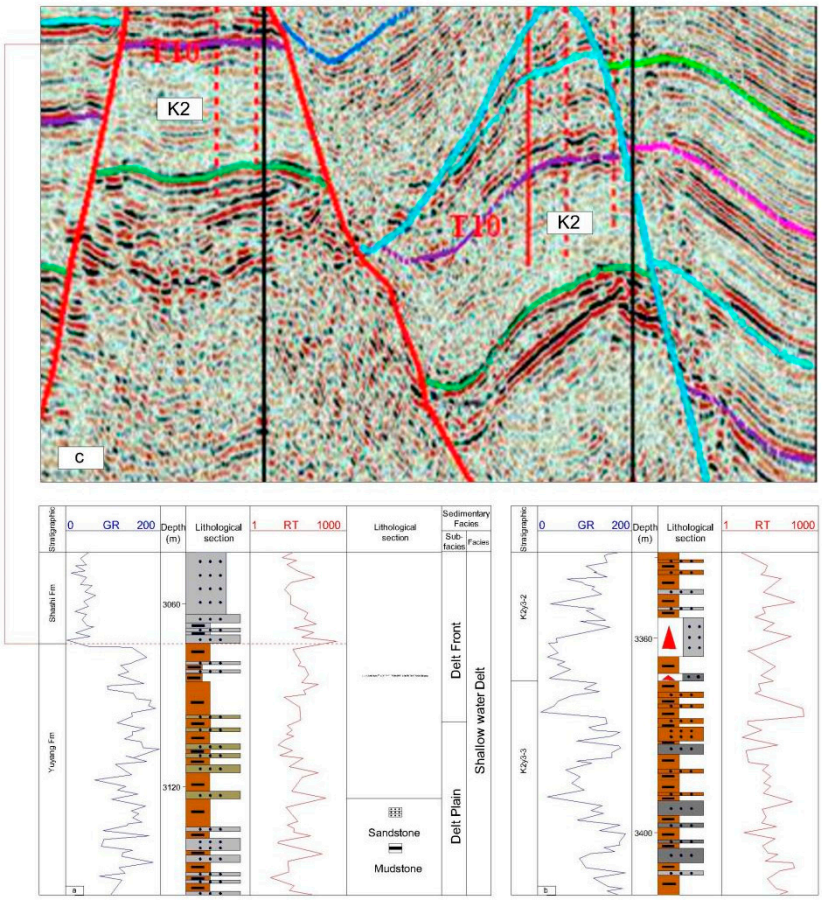

Figure 6. Lithologic and electrical characteristics of Upper Yu yang Formation and sequence interface at Top of Well SK10; (**a**) Seismic profile; (**b**) Yu yang Formation; (**c**) Sha shi.Formation.

3.2.2. Logging Curve Mark

According to the morphological characteristics of the logging curve, it can be used to identify the vertical sedimentary sequence. The top-bottom contact relationship can be divided into two types: abrupt change and gradual change, which are mainly used to reflect the changes in the sedimentary environment and hydrodynamic conditions in the study area. The abrupt changes and gradients among box, linear, and finger on the logging curve correspond to different types of sedimentary microfacies. The corresponding

relationship between the short-term cycle and the logging curve is established to guide the division of high-resolution sequences in the whole region.

The transformation of mudstone sequence and stratigraphic sequence is a kind of response curve recorded on the basis of stratigraphic sequence and flood surface. Therefore, on the logging curve, on the one hand, the para-sequence boundary can be identified according to the low resistivity and high natural gamma ray characteristics of flood mudstone, on the other hand, the transformation of the logging curve style can also be used as a reference. Using a logging curve to identify the conversion point of the base level cycle is usually based on the calibration of the coring well section, using the coring well section to establish the logging response model of the short-term base level cycle and conversion interface to guide the cycle division on regional non-coring wells.

3.3. Seismic Wave Profile Data of Wells and High-Resolution Sequence Stratigraphy Division Method

3.3.1. Seismic Wave Profile Data of Wells

The energy and frequency of seismic data in the Jiang ling Depression Complex I fault block area of the Jiang han Basin are very much influenced by tectonics, producing strong scattering noise, and the signal energy and frequency decay quickly with increasing depth, resulting in large spatial differences in seismic data frequency and amplitude. For the imaging study of seismic data of SK8-9 well (see Figure 7), through the high-density model orientation seismic profile, fruit profile signal-to-noise ratio, high resolution, good wave group characteristics, reliable tectonic morphology, clear fracture, especially the main target layer seismic reflection characteristics, clear, seam hole body imaging accuracy improved, providing reliable seismic data for the remaining oil reservoir prediction and trap closure implementation in this area.

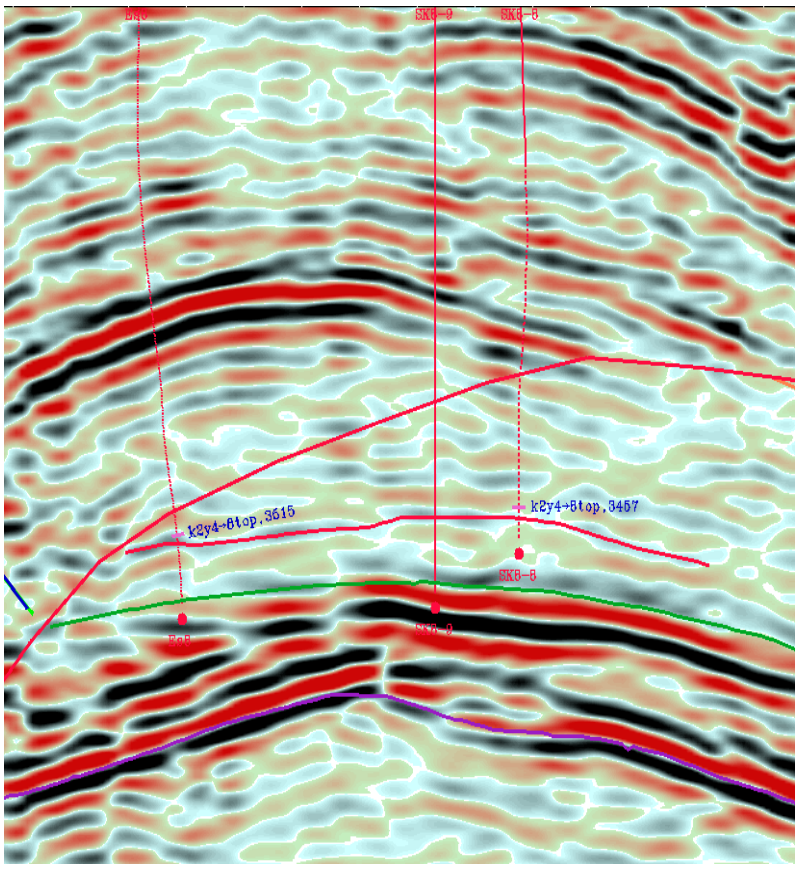

Figure 7. Seismic profile of SK8-9 well.

3.3.2. High Resolution Sequence Stratigraphy Division Method

The seismic reflection boundary is isochronous or parallel to the stratum, which can be used for base-level cycle analysis. However, since the frequency band width of the conventional seismic reflection wave is only about 8–60 Hz, and the distinguished stratum is far greater than the thickness of the para-sequence, it can only be used to identify long-term base level cycles.

Usually, the transition position of the medium- and long-term base-level cycles from fall to rise is consistent with the formation period of the sequence boundary. The seismic profile shows that the seismic reflection termination type of regional distribution or reflecting the uncoordinated relationship of strata corresponds to the maximum flood level, which represents the conversion position from the rise of the base-level cycle to the decline, which represents the maximum period of accommodation space and corresponds to the strong amplitude continuous reflection boundary on the stratigraphic profile. Therefore, a stratigraphic sequence can be divided into two terms, medium and long, on the seismic reflection profile, including the rising hemicycle and falling hemicycle.

However, according to the changes in seismic reflection configuration in medium- and long-term base-level cycles, combined with the characteristics of stratigraphic superposition style observed by logging curves and cores, the composition of high-frequency cycles can be predicted, and the correlation of horizontal high-frequency sequences can be guided. The identification and grade analysis of the base-level cycle interface is the key to multi-stage stratigraphic comparison with the stratigraphic base level as the reference frame. Like the stratigraphic features in marine stratigraphic stratigraphy, the base-level cycle also has multistage features that can be divided into multistage long-term cycles, medium-term cycles, short-term cycles, and so on.

In the sequence boundaries, flooding surfaces of various scales are often developed. The flood surface in the study area is mostly represented by thick mudstone deposition on the drilling and logging sections, which is the conversion interface between retrogradation and progradation. In an earthquake, it is a mostly strong reflection with good continuity, and some superelevation phenomena can be seen. Taking the maximum flooding surface between the two sequence boundaries as the boundary, one sequence can be divided into medium- and short-term cycles of base-level rise and fall. Taking the change in short-term base-level cycle as the basic unit of sedimentary microfacies analysis, drilling, logging, and seismic sequence data can be divided on the basis of determining the sequence boundary. By synthesizing seismic records, the relationship between well and seismic data can be established. Based on the fine core observation and description of 18 typical coring wells, combined with regional seismic reflection characteristics, logging, and recording signs, the Cretaceous Yu yang formation is divided into 5 medium-term base-level cycles (MSC2–MSC6) and 17 short-term base-level cycles (Figure 8).

3.4. Short-Term Cycle Structural Style Data

3.4.1. Short-Term Cycle Structure Style

The short-term cycle can be divided into intermittent exposures, scouring interrupted surfaces, and lithologic abrupt change surfaces as the identification mark of the stratigraphic boundary, which summarizes the short-term cycle development pattern in the study area (Figure 9). Taking the flood plan as the symmetry axis, the structure can be divided into three subtypes according to the variation relationship of the thickness of two different time units: ① Asymmetrical structure dominated by a rising hemicycle (E1, E2, E3); ② competent symmetrical structure dominated by a rising-falling hemicycle (F2); or ③ incompetent symmetrical structure dominated by rising or falling hemicycle (F1, F3).

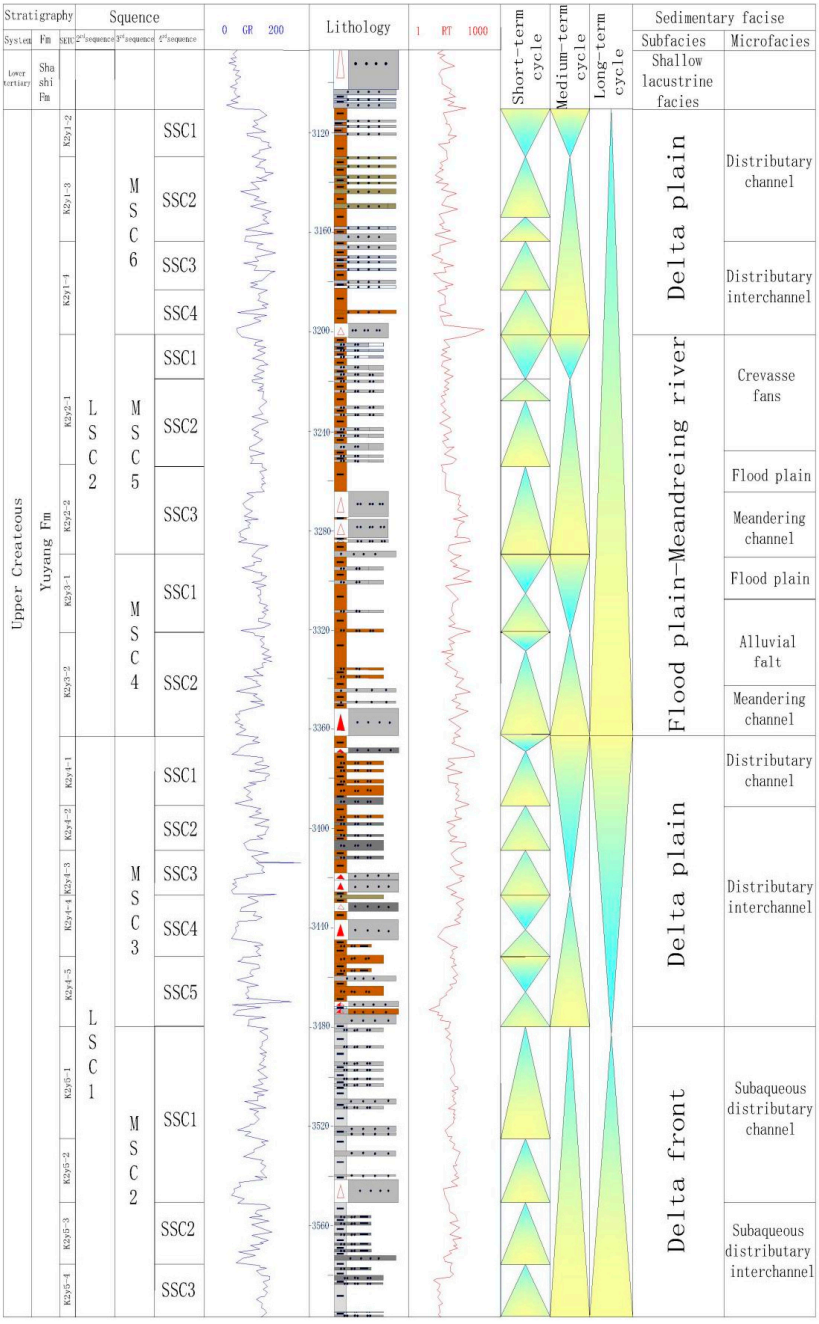

Figure 8. High-resolution sequence stratigraphy and sedimentary facies column of Cretaceous Yu yang Formation in Jiangling Depression.

There is a certain correspondence between the short-term base-level cycle and sedimentary facies development. In the study area, a set of fluvial-deltaic facies systems are mainly developed, and the rise and fall of the datum surface in different sedimentary facies belt development environments has different records in the process of stratigraphic deposition; for instance, different facies markers have different depositional characteristics. The rising hemicycle sedimentary microfacies assemblages are mostly meandering channel-alluvial plain, distributary channel-flood deposition, and submerged divergent channel-tributary bay, which represent an upward thinning positive rhythmic cycle recession sequence; the falling hemicycle sedimentary microfacies assemblages are mostly alluvial plain. The downward semi-rotational sedimentary microfacies assemblages are mostly alluvial plains–underwater crevasse fans, floodplain sediments-underwater crevasse

fans, and underwater crevasse fans-subaqueous distributary channels, which represent upward coarsening anti-rhythmic cycle accretion sequences.

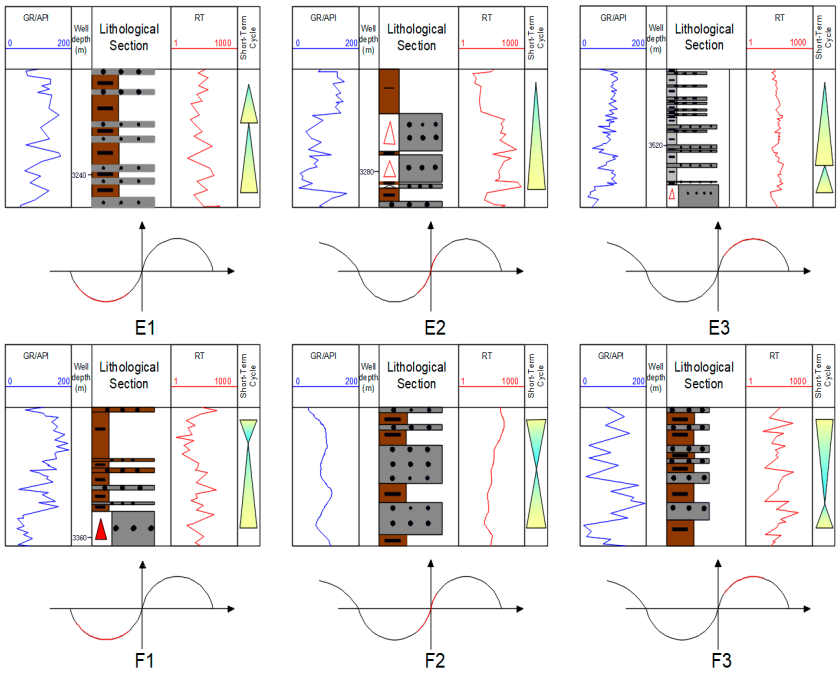

Figure 9. The styles of Cretaceous short-term base-level cycle in Jiang ling Depression.

3.4.2. High-Resolution Sequence Division Scheme

The key stratigraphic section in the Song zi area is the Upper Cretaceous Yu yang Formation, and the bottom boundary of the oil formation at the bottom of the Paleozoic Sha shi Formation is used as the top boundary of the target layer. Based on the lithology, logging curve, and short-term base-level cycle development style, a stratigraphic classification scheme was established in the Song zi area (Figure 8).

The Yu yang Formation is divided into 5 medium-term cycles (MSC6-MSC5-MSC4-MSC3-MSC2) and 17 short-term cycles. From Section 1 to Section 5 of the Yu yang formation, a set of meandering rivers, shallow water delta plains, and delta front sedimentary systems composed of brownish-red, grayish-green mudstone, grayish-white siltstone, and fine sandstone are developed, respectively. The first section of the Yu yang Formation is divided into one medium-term cycle (MSC6) and four short-term cycles (SSC1- SSC4). The second section of the Yu yang Formation is divided into one medium-term cycle (MSC5) and three short-term cycles (SSC1- SSC3). The third section of the Yu yang Formation is divided into one medium-term cycle (MSC4) and two short-term cycles (SSC1- SSC2). The fourth section of the Yu yang Formation is divided into one medium-term cycle (MSC3) and four short-term cycles (SSC1- SSC4). The fifth section of the Yu yang Formation is divided into one medium-term cycle (MSC2) and three short-term cycles (SSC1- SSC3). The whole section of the Yu yang Formation is gradually transformed from an asymmetrical structure dominated by a rising hemicycle (E2) to an incompetent symmetrical structure dominated by a rising-falling hemicycle (F2) and an incompetent symmetrical structure dominated by a rising hemicycle (F1).

3.4.3. Sand Body Development Rule Controlled by Base-Level Cycle

According to the corresponding relationship between the above cycle structure, sedimentary facies, and logging curve (Figure 10), it is considered that the development style of the short-term base-level cycle reflects the lithology, logging curve, sedimentary facies development sequence, and combination characteristics, and the development type of

the channel sand body corresponding to the short-term base-level cycle style in different periods is different (Figure 11).

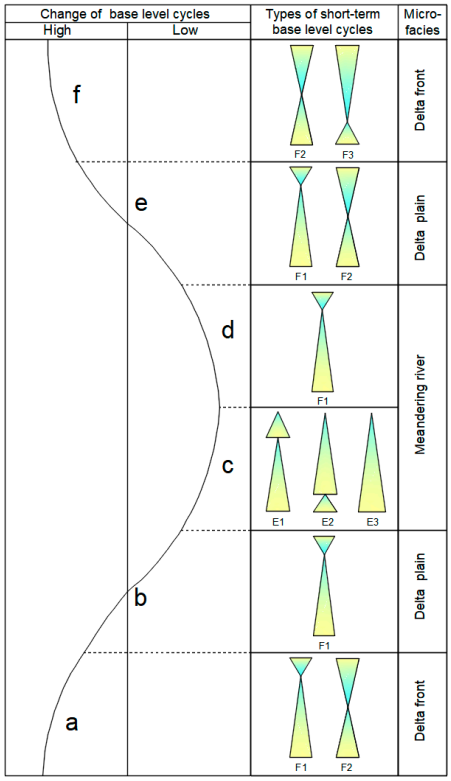

Figure 10. Development types and characteristics of reservoir sand bodies controlled by Cretaceous base-level cycles in Jiang ling.

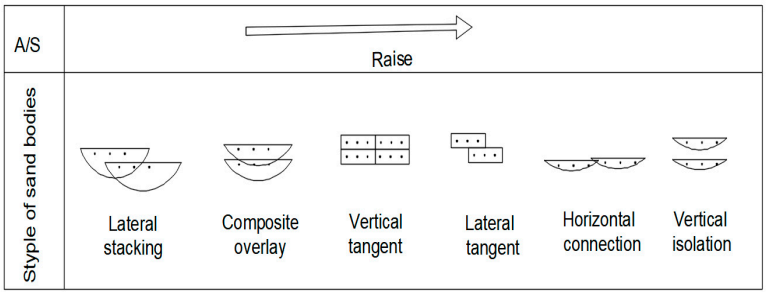

Figure 11. Development pattern of channel sand body controlled by Cretaceous A/S in Jiang ling Depression.

The rise and fall of base level have a direct impact on the sedimentary development of sand bodies and the level of development of cycles. According to the change law of base-level rise and fall and the accommodation space value increase and decrease rate, the development process of the medium-term cycle is divided into three stages: accelerated decline (a), slow decline to the lowest point and then slowly rising (c–d), and rapid rise and then slowly rise to the highest (e–f). The short-term cycles of each stage show different superposition patterns and indicate the development characteristics of different channel sand bodies.

The short-term base-level cycles in the accelerated fall e stage and the rapid rise b stage develop incomplete symmetry types or nearly complete symmetry types (F1, F2) dominated by the rising hemicycle. At this stage, the shallow water delta plain deposits are mainly developed in the study area, and the distributary channel sand bodies are very developed; in the c-d stage, the short-term base-level cycle develops an upward

"deepening" asymmetric type (E, F1). At this stage, it is a typical meandering river facies deposition, and the reservoir sand body is a meandering river sand body; in the short-term base-level cycle of the e-f stage, incomplete symmetry types or nearly complete symmetry types (F2, F3) dominated by falling hemicycles are developed. At this stage, underwater shallow delta front sedimentation has mainly developed in the study area, and the sand body type is mainly a subaqueous distributary channel sand body.

4. Results

4.1. Mineral Composition Results

Based on the mineral composition triangle (Figure 12), it can be concluded that the K_2y reservoir is mainly feldspathic quartz sandstone and fine-grained rock chip quartz sandstone. Quartz is the main inorganic mineral component, and the variation in its relative composition affects the mechanical properties of the rock, its pore structure, and its ability to adsorb gases. In shale with low organic carbon content, quartz, with larger pore generation, retains and stores a large of hydrocarbons. It can be concluded from the analysis of the mineral composition triangulation study that the oil permeability of the area is better.

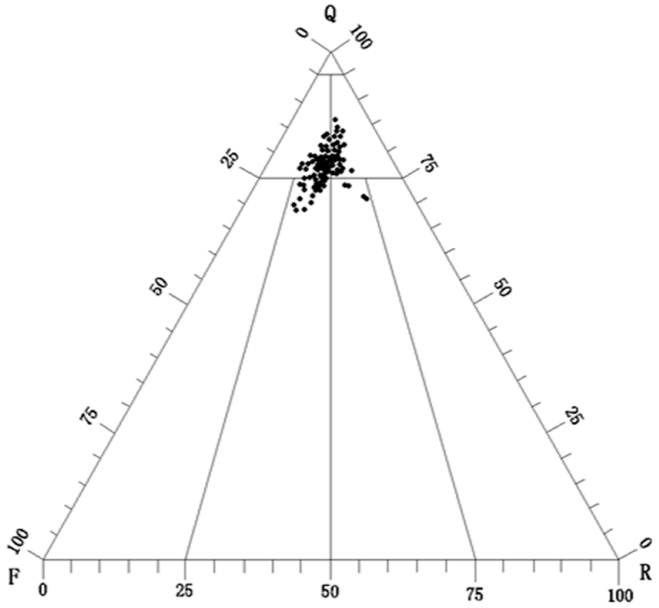

Figure 12. Triangle diagram of K_2y mineral composition in Well SK10.

4.2. Results of Pore Structure

According to the pore structure, cast thin section, and electro-ytterbium scan data of a large number of statistics (Figure 13), we can draw the following conclusions: The reservoir pore diameter of the Yu yang Formation is generally in the range of 10–70 m, of which 10–30 m pore size distribution is the most frequent, and the pore size distribution is more concentrated. Additionally, the throat channel is small: The average throat radius distribution is 0.5–1 m, the maximum throat radius is 2 m, and the average radius of the main flow throat is about 1.5 m. According to the criteria for the division of the pore throat, it should be classified as a fine throat-micro-throat structure.

Frequency diagram of pore size distribution in Fu 1 Fault Block.

The pore size distribution of the reservoir is single-peaked (Figure 14), and the pore radius is mainly distributed in the range of 10–20 m, accounting for 27.625% of the total pore area. With the increase of the pore radius, the area percentage becomes increasingly smaller, showing a one-sided downward trend.

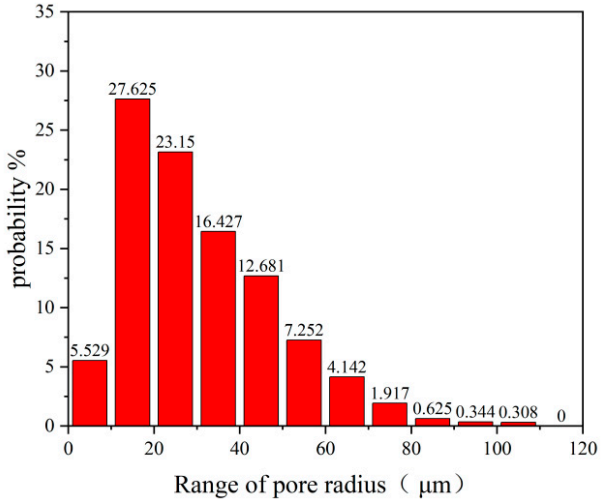

Figure 13. Distribution Frequency Map of Pore Size of Cretaceous Reservoir in Fu 1 Fault Block.

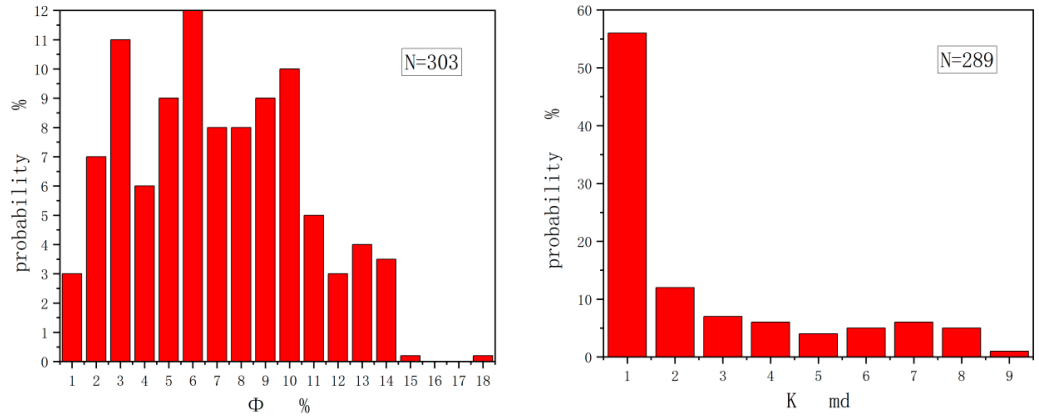

(**a**) (**b**)

Figure 14. Histogram of porosity distribution and permeability distribution in the Fu 1 fault block: (**a**) Histogram of porosity distribution; (**b**) Histogram of permeability distribution.

4.3. Scanning Results of Cast Thin Sections and Ytterbium

Scanning electron microscopy and cast thin section samples (Figure 15) collected from the oil and gas formation show that the pore types in the oil and gas formation are intergranular dissolved pore and micro-fissure, and usually, the higher the content of inter-grain pores in clastic reservoirs, the better the reservoir physical properties. The distribution state of the remaining oil and water in the pore space is divided into three types by SEM and cast thin section samples. The first is the bound state, with remaining oil adsorbed on the mineral surface as shown in (Figure 15a,b); the second is the free state (Figure 15c), where there is intra-grain, light mist, inter-grain adsorbed and cluster remaining oil; the third is the semi-bound state, with residual oil in the outer layer of the bound state type or far from the mineral surface (Figure 15d), with precipitated, corner, and throat residual oil in the pores.

4.4. Residual Oil Connectivity Results

According to the comparison of oil layers (Figure 16), the formation location of well SK8-5 is the highest (3446 m), well SK8-8 is the second highest (3464 m), and wells ES8 and ES14 are lower (3520 m). From the analysis of the well SK8 and ES14 oil and gas results, the two wells are also the oil formation of the Yu yang Group 4 oil formation group; their physical properties are comparable, but the high part (about 60 m high) of wells SK8-5 and SK8-8 were tested as oil-bearing water layer, while wells ES8 and ES14 produce pure oil

and stable production, and the logs are interpreted as oil formation. Therefore, wells SK8-8 and SK8-5 do not belong to the same reservoir as wells ES8 and ES14, and there should be a blocking layer between them. The 3D seismic data show that there is a superposition relationship between the phase axis, so they are two unconnected reservoirs. The design well location SK8-9 falls on the side of well ES14.

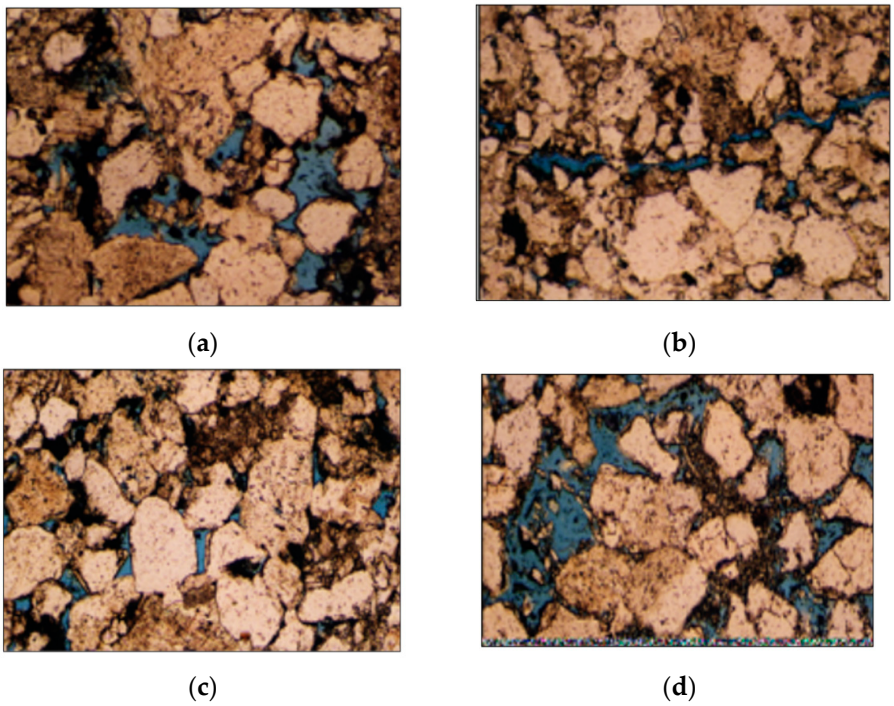

Figure 15. Scanning electron microscopy and cast sheet samples: (**a**) intergranular dissolved pore; (**b**) micro-fissure; (**c**) primary intergranular porosity; (**d**) casting mold-intergranular dissolved pore.

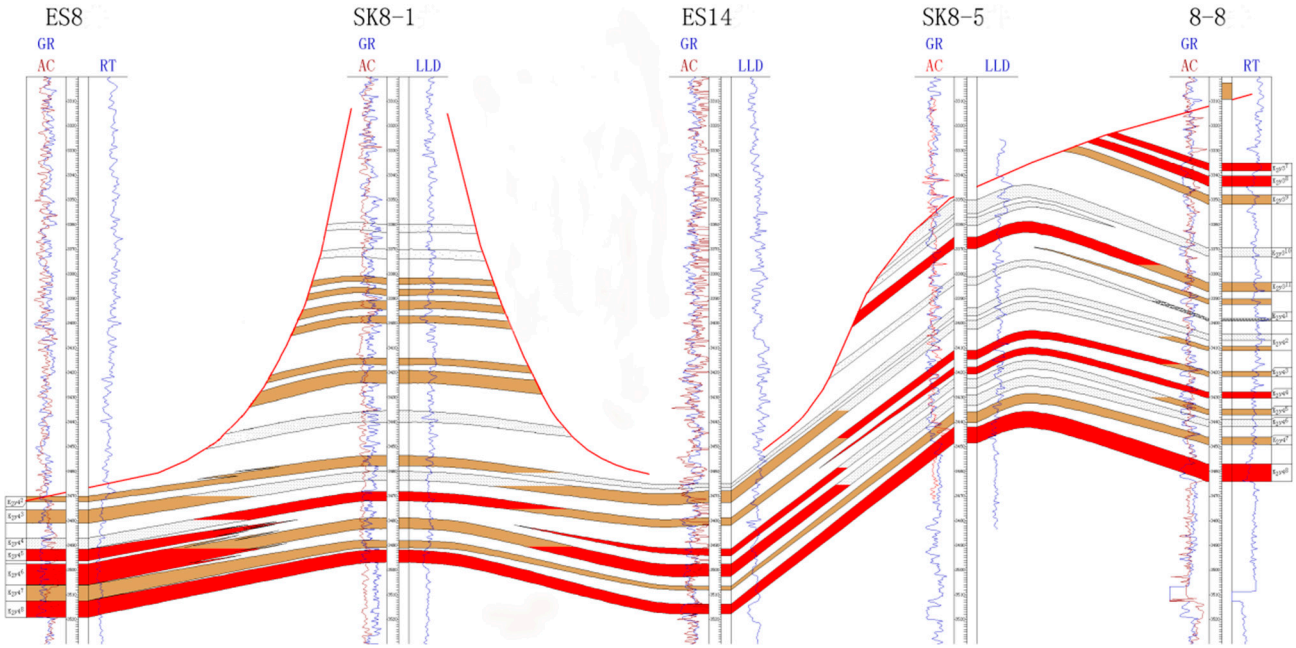

Figure 16. Profile of well connection in Fu I fault block.

The Fu I fault block corresponds to 3513.6–3520.4 m oil formation of K_2y4 oil formation of Cretaceous Yu yang Group in E Shen 14 well, 3487.0–3520.0 m oil formation of K_2y4

oil formation of Cretaceous Yu yang Group in ES8 well and 3457–3464 m oil formation in SK8-8 well.

The trap implementation of the Yu yang Formation in the Fu I fault block is reliable and complete; most of the oil test results for the neighboring wells have reached the industrial oil flow standard. The site of the designed development preparation well EZ8-9 falls within the overlap zone of K_2y1, K_2y2, K_2y3, and K_2y4 sandstone percentages; the most developed direction of the sand body is northwest; the most productive well is also within the above direction, close to the Wan cheng–Xie Fengqiao fault and the fracture-associated well. At the same time, the proximity to the oil source gives the opportunity to capture the oil first, which makes it easy to obtain high-yielding oil streams.

According to the data for the drilled well K_2y4 of the Yu yang Formation in the complex I fault block, the oil layer thickness connectivity ratio (i.e., the ratio of oil layer connectivity thickness to total sand layer thickness) in the oil-bearing area is 84.4%, and the layer number (8) connectivity ratio is 60%, so the connectivity condition is relatively good.

5. Discussion

This paper focuses on the western part of the Jiangling Depression in the Jianghan Basin. Based on drilling, core, logging, seismic, and production data based on the changes of base-level cycles in sequence stratigraphy, the direction of reservoir extension is clarified, and the allocation of production wells is effectively guided by the comparative analysis of reservoir fine connectivity and the configuration relationship of production wells, which greatly promotes the sustainable development of remaining oil.

5.1. Discussion on Plane Development of Short-Term Cycles

From the short-cycle microfacies configuration and sand body distribution of the Yu yang formation, it can be seen that the base-level fluctuation restricted by structure, climate, and provenance during the sedimentary period of the Yu yang formation is the main controlling factor of the third-order sequence structure in this area. The sedimentary cycle of the Yu yang formation is an asymmetric cycle dominated by sedimentary in the base-level rise period. It is composed of six medium-term cycles. During the base-level rise period, the accommodation space in the central and western regions of the Fu I fault block (near SK8-4-1 well) is high, the sediment accumulation and preservation capacity are strong, and the stratigraphic sedimentary thickness is significantly greater than that in other regions. It is mainly meandering channel facies. From the distribution direction of sand bodies in the short-term cycles SSC3-1 to SSC4-3, from bottom to top, the river direction has a trend of migration from northwest to north. During the short decline period of the base level, the accommodation space of the high part of the northern gentle slope is reduced, the sediment accumulation and retention potential are small, and the road scouring often occurs, forming the scouring erosion surface. A large number of sediments are transported to the south, resulting in river progradation. The syn-sedimentary process is reflected as follows: The cyclic strata dominated by flood plain flood lake facies in the lower part of the eastern structural slope break in the base-level rising period, and the strata dominated by meandering channel in the upper part are the same isochronous interface, while the sedimentary discontinuity in the upper part of the slope break without sedimentary strata in the base-level falling period is an isochronous interface.

5.2. Discussion on Influence of Sand Structure on Residual Oil Distribution under River Extension

The study shows that the Yu yang Formation of the Cretaceous developed a flexural river-deltaic sedimentary system and other petrographic types, forming a non-homogeneity along and thus affecting the distribution of remaining oil. In the western part of the Xie Fengqiao fault, the alluvial-flood plain sand body is mainly developed at the high fault stage; the Fu Xingchang fault block develops the curvilinear river-deltaic sedimentary sand body, and the area west of Xie Fengqiao mainly develops the submarine divergent river sand body at the front edge of delta.

The remaining oil of the Yu yang Formation is mainly distributed in the submarine diversion channel and natural dike sedimentary microfacies and less in the side beach, mud ping and sand ping. The submarine diversion channel microfacies has the best physical properties; the remaining oil content is generally more than 35%. The submarine diversion channel sand body has high physical properties and high original oil saturation and has the advantage of thicker sand body compared with the marginal facies, which still has quite objective remaining oil potential.

6. Conclusions

(1) The comparative analysis of high-resolution stratigraphic sequences from drilling and logging data shows that the Yu yang Formation of the Cretaceous is divided into 5 medium-term cycles (MSC6-MSC5-MSC4-MSC3-MSC2) and 17 short-term cycles (SSSC17-SSC1). The Yu yang Formation mainly develops a set of brown-red and gray-green mudstones and gray-white powdery fine sandstone composed of meandering rivers and shallow-water delta plains and delta front sedimentation systems. The whole section of the Yu yang Formation is gradually transformed from an asymmetrical structure dominated by a rising hemicycle (E2) to an incompetent symmetrical structure dominated by a rising–falling hemicycle (F2) and an incompetent symmetrical structure dominated by a rising hemicycle (F1).

(2) The study of sedimentary system evolution shows that the Cretaceous Yu yang formation in this belt develops meandering river delta sedimentary systems and other lithofacies types. Alluvial flood plain sand bodies are mainly developed in the high fault stage in the west of Xie Fengqiao fault; meandering river delta sedimentary sand bodies are developed in the Fu xing chang fault block, and underwater distributary channel sand bodies in the delta front developed mainly in the west of Xie Fengqiao.

(3) Identifying different types of reservoirs according to the tectonic position and development sequence combined with the data statistics of the drilled wells in K_2y4 of Yu yang Formation in the complex I fault block, it is found that the thickness connectivity ratio (i.e., the ratio of the connectivity thickness of oil layer to the total thickness of sand layer) in the oil-bearing area is 84.4%, and the number of layers (8) was 60%.

Author Contributions: Conceptualization, W.Z. and M.S.; methodology, W.Z.; software, W.Z.; validation, W.Z. and M.S.; formal analysis, W.Z.; investigation, W.Z., Y.Q. and K.L.; resources, W.Z.; data curation, W.Z.; writing—original draft preparation, W.Z.; writing—review and editing, W.Z.; visualization, M.S.; supervision, W.Z.; project administration, S.D.; funding acquisition, S.D. All authors have read and agreed to the published version of the manuscript.

Funding: This work was funded by the Open Foundation of Key Laboratory of Coal Exploration and Comprehensive Utilization of Ministry of Natural Resources, grant number KF2021-5, and the National Key R&D program of China, grant numbers 2018YFC0807801 and 2018YFB0605503.

Institutional Review Board Statement: Not applicable.

Informed Consent Statement: Not applicable.

Data Availability Statement: Data is contained within the article.

Acknowledgments: We would like to thank the reviewers for their valuable comments and efforts.

Conflicts of Interest: The authors declare no conflict of interest.

References

1. Catuneanu, O. *Principles of Sequence Stratigraphy*; Elsevier: Amsterdam, The Netherlands; Boston, MA, USA; Heidelberg, Germany, 2006.
2. Zecchin, M.; Catuneanu, O. High-resolution sequence stratigraphy of clastic shelves I: Units and bounding surfaces. *Mar. Pet. Geol.* **2013**, *39*, 11–25. [CrossRef]
3. Mitchum, R., Jr.; Vail, P.; Thompson, S., III. Seismic stratigraphy and global changes of sea level: Part 2. The depositional sequence as a basic unit for stratigraphic analysis: Section 2. Application of seismic reflection configuration to stratigraphic interpretation.

In *Seismic Stratigraphy Applications to Hydrocarbon Exploration*; Payton, C.E., Ed.; American Association of Petroleum Geologists: Tulsa, OK, USA, 1997; pp. 53–62.
4. Posamentier, H.; Jervey, M. Eustatic controls on clastic deposition I—Conceptual framework. In *Sea-Level Changes: An Integrated Approach*; Wilgus, C., Hastings, B.S.C., Kendall, C.G., Posamentier, H.W., Ross, C.A., Van Wagoner, J.C., Eds.; SEPM Special Publication 42; SEPM Society for Sedimentary Geology: Tulsa, OK, USA, 1988; pp. 109–124.
5. Posamentier, H.W.; Morris, W.R. Aspects of the stratal architecture of forced regressive deposits. *Geol. Soc. Spec. Publ.* **2000**, *172*, 19–46. [CrossRef]
6. Hardenbol, J. An overview of the fundamentals of sequence stratigraphy and key definitions. In *Sea-Level Changes: An Integrated Approach*; Wilgus, K.C., Ed.; Society of Economic Paleontologists and Mineralogists: Tulsa, OK, USA, 1988; pp. 39–45.
7. Van Wagoner, J.C.; Mitchum, R. *Siliciclastic Sequence Stratigraphy in Well Logs, Cores, and Outcrops: Concepts for High–Resolution Correlation of Time and Facies*; American Association of Petroleum Geologists: Tulsa, OK, USA, 1990; pp. 3–55.
8. Henry, W.; Posamentier, P.W. Siliciclastic Sequence Stratigraphy and Petroleum Geology—Where to From Here ? *AAPG Bull.* **1993**, *77*, 731–742.
9. Van Wagoner, J.C.; Mitchum, R.M. Siliciclastic sequence stratigraphy in well logs, cores and outcrops. In *AAPG Methods in Exploration*; American Association of Petroleum Geologists: Tulsa, OK, USA, 1997; Volume 7.
10. Cross, T.A.; Lessenger, M.A. Sediment Volume Partitioning: Rationale for Stratigraphic Model Evaluation and High—Resolution Stratigraphic Correlation. In Proceedings of the Norwegian Petroleum Society Conference, Stavanger, Norwegian, 6–8 September 1995.
11. Ray, S.; Chakraborty, T. Lower Gondwana fluvial succession of the Pench–Kanhan valley, India: Stratigraphic architecture and depositional controls. *Sediment. Geol.* **2002**, *151*, 243–271. [CrossRef]
12. Smith, G.H.S.; Ashworth, P.J. The sedimentology and alluvial architecture of the sandy braided South Saskatchewan River, Canada. *Sedimentology* **2006**, *53*, 413–434. [CrossRef]
13. Han, Z.Z.; Yang, R.C. Remaining oil distribution in Ng33 bottom water reservoir of Lin 2–6 fault-block in Huimin depression and potential tapping in horizontal well. *Min. Sci. Technol.* **2009**, *19*, 102–107. [CrossRef]
14. Ghazi, S.; Mountney, N.P. Facies and architectural element analysis of a meandering fluvial succession: The Permian Warchha sandstone, salt range, Pakistan. *Sediment. Geol.* **2009**, *221*, 99–126. [CrossRef]
15. Katherine, L.M.; Andrea, F. Punctuated deep-water channel migration: High-resolution subsurface data from the Lucia Chica channel system, offshore California, USA. *J. Sediment. Res.* **2012**, *82*, 1–8.
16. Weissmann, G.S.; Hartley, A.J. Fluvial form in modern continental sedimentary basins: Distributive fluvial systems. *Geology* **2010**, *28*, 39–42. [CrossRef]
17. Li, Z.P.; Lin, C.Y. An internal structure model of subaqueous distributary channel sands of the fluvial-dominated delta. *Acta Pet. Sin.* **2012**, *33*, 101–105.
18. Kukulski, R.B.; Moslow, T.F. Tight gas sandstone reservoir delineation through channel-belt analysis, Late Jurassic Monteith Formation, Alberta Deep Basin. *Bull. Can. Pet. Geol.* **2013**, *61*, 133–156. [CrossRef]
19. Hartley, A.J.; Weissmann, G.S. Large distributive fluvial systems: Characteristics, distribution and controls on development. *J. Sediment. Res.* **2010**, *80*, 167–183. [CrossRef]
20. Rodrigues, S.; Mosselman, E. Alternate bars in a sandy gravel bed river:Generation, migration and interactions with superimposed dunes. *Earth Surf. Process. Landf.* **2015**, *40*, 610–628. [CrossRef]
21. Yang, S.C.; Zhao, X.D. Inner heterogeneity within braided bar of braided river reservoir and its influence on remaining oil distribution. *J. Cent. South Univ. (Sci. Technol.)* **2015**, *46*, 1066–1074.
22. Fu, X.F.; Lan, X. Characteristics of fault zones and their control on remaining oil distribution at the fault edge: A case study from the northern Xingshugang Anticline in the Daqing Oilfield, China. *Pet. Sci.* **2016**, *13*, 418–433. [CrossRef]
23. Brian, R.T.; Gillian, N.T. The Table Rocks Sandstone: A fluvial, friction-dominated lobate mouth bar sandbody in the Westphalian B Coal Measures, NE England. *Sediment. Geol.* **2006**, *190*, 97–119.
24. Li, S.L.; Ma, Y.Z. Change of deltaic depositional environment and its impacts on reservoir properties–A braided delta in South China Sea. *Mar. Pet. Geol.* **2014**, *58*, 760–775. [CrossRef]
25. Li, W.; Bhattacharya, J.P. Temporal evolution of fluvial style in a compound incised-valley fill, Ferron "Notom Delta" Henry Mountains region, Utah (U.S.A.). *J. Sediment. Res.* **2010**, *80*, 529–549. [CrossRef]
26. Aqeel, A.M.; Shi, S.M. Study of distribution of remaining oil in West Block of the Third District in North Saertu. *Earth Sci. Res. J.* **2016**, *20*, 2.
27. Hiranya Sahoo, M.; Royhan Gani, G.J. Facies- to sandbody-scale heterogeneity in a tight-gas fluvial reservoir analog: Blackhawk Formation, Wasatch Plateau, Utah, USA. *Mar. Pet. Geol.* **2016**, *78*, 48–69. [CrossRef]
28. Chen, L.; Lin, Z.P. Analysis of Reservoir Architecture of Shallow-water Delta Front Based on Process—A Case of S2L410 in Southern 79 Block in Wennan Oilfield. *Stud. Eng. Technol.* **2017**, *4*, 1. [CrossRef]
29. Gao, S.; Chen, S.M. Fine characterization of large composite channel sandbody architecture and its control on remaining oil distribution: A case study of alkaline-surfactant—polymer (ASP) flooding test area in Xingshugang oilfield. *J. Pet. Sci. Eng.* **2019**, *175*, 363–374. [CrossRef]

30. Zang, D.S.; Bao, Z.D. Sandbody architecture analysis of braided river reservoirs and their significance for remaining oil distribution: A case study based on a new outcrop in the Songliao Basin, Northeast China. *Energy Explor. Exploit.* **2020**, *38*, 2231–2251. [CrossRef]
31. Yu, Y.; Zhang, C.M. Sedimentary characteristics and genetic mechanism of a deep-water channel system in the Zhujiang Formation of Baiyun Sag, Pearl River Mouth Basin. *Deep-Sea Res. Part I–Oceanogr. Res. Pap.* **2021**, *168*, 103456. [CrossRef]
32. Yu, Y.; Cai, L.H. Sedimentary Sequence, Evolution Model and Petroleum Geological Significance of Forced Regression: A Case Study of the Miocene Zhujiang Formation of the Pearl River Mouth Basin in the Northern South China Sea. *J. Mar. Sci. Eng.* **2021**, *9*, 1298. [CrossRef]
33. Yu, Y.; Zhang, C.M. Sedimentary facies characterization of forced regression in the Pearl River Mouth basin. *Open Geosci.* **2022**, *14*, 208–223. [CrossRef]
34. Liu, H.; Xia, Q.L. Geologic-seismic models, prediction of shallow-water lacustrine delta sandbody and hydrocarbon potential in the Late Miocene, Huanghekou Sag, Bohai Bay Basin, northern China. *J. Palaeogeogr.* **2018**, *7*, 66–87. [CrossRef]
35. Marco, S.L.; Lin, C.Y. Seismic sedimentology of lacustrine delta-fed turbidite systems: Implications for paleoenvironment reconstruction and reservoir prediction. *Mar. Pet. Geol.* **2020**, *113*, 104159.
36. José, M.P.; Nicolás, F. Sedimentology and alluvial architecture of the Bajo Barreal Formation (Upper Cretaceous) in the Golfo San Jorge Basin: Outcrop analogues of the richest oil-bearing fluvial succession in Argentina. *Mar. Pet. Geol.* **2016**, *72*, 317–335.
37. Li, Y.; Fan, A.P. Braided deltas and diagenetic control on tight sandstone reservoirs: A case study on the Permian Lower Shihezi Formation in the southern Ordos Basin (central China). *Sediment. Geol.* **2022**, *435*, 106156. [CrossRef]
38. Martini, I.; Sandrelli, F. Facies analysis of a Pliocene river-dominated deltaic succession (Siena Basin, Italy): Implications for the formation and infilling of terminal distributary channels. *Sedimentology* **2015**, *62*, 234–265. [CrossRef]
39. Lariu, C.; Bhattacharya, J.P. Interplay between river discharge and topography of the basin floor in a hyperpycnal lacustrine delta. *Sedimentology* **2012**, *59*, 704–728.
40. Olariu, C.; Steel, R.J. Delta-front hyperpycnal bed geometry and implications for reservoir modeling: Cretaceous Panther Tongue delta, Book Cliffs, Utah. *AAPG Bull* **2010**, *94*, 819–845. [CrossRef]
41. Schomacker, E.R.; Kjemperud, A.V. Recognition and significance of sharpbased mouth-bar deposits in the Eocene Green River Formation, Uinta Basin, Utah. *Sedimentology* **2010**, *57*, 1069–1087. [CrossRef]
42. Sun, Y.H.; Wang, Q. Sedimentary microfacies of the second member of Shuangyang Formation in Changchun oilfield, Yitong Basin, China. *Fresenius Environ. Bull.* **2019**, *28*, 7.
43. Zhong, Y.; Zhou, L. Characteristics of depositional environment and evolution of Upper Cretaceous Mishrif Formation, Halfaya Oil field, Iraq based on sedimentary microfacies analysis. *J. Afr. Earth Sci.* **2018**, *140*, 151–168. [CrossRef]
44. Zhang, X.J.; Wu, D. Controls of sandstone architecture on hydrocarbon accumulation in a shallow-water delta from the Jurassic Shaximiao Formation of the western Sichuan Basin in China. *Energy Rep.* **2022**, *8*, 6068–6085. [CrossRef]
45. Wu, D.; Zhao, D. Sedimentology and seismic geomorphology of a lacustrine depositional system from the deep zone of the Gaoyou Sag, Subei Basin, eastern China. *Aust. J. Earth Sci.* **2017**, *64*, 265–282. [CrossRef]
46. Cao, T.T.; Liu, H. Pore evolution in siliceous shales and its influence on shale gas-bearing capacity in eastern Sichuan-western Hubei, China. *J. Pet. Sci. Eng.* **2022**, *208*, 109597. [CrossRef]
47. Cao, T.T.; Deng, M. Pore formation and evolution of organic-rich shale during the entire hydrocarbon generation process: Examination of artificially and naturally matured samples. *J. Nat. Gas Sci. Eng.* **2021**, *93*, 104020. [CrossRef]
48. Cao, T.T.; Xu, H. Factors influencing microstructure and porosity in shales of the Wufeng-Longmaxi formations in northwestern Guizhou, China. *J. Pet. Sci. Eng.* **2020**, *191*, 107181. [CrossRef]
49. Cao, T.T.; Deng, M.; Hursthouse Andrew, S. Characteristics and controlling factors of pore structure of the Permian shale in southern Anhui province, East China. *J. Nat. Gas Sci. Eng.* **2018**, *60*, 228–245. [CrossRef]
50. Liao, J.P.; Liu, H.X. 3-D Butterworth filtering for 3-D high-density onshore Seismic Field Data. *J. Environ. Eng. Geophys.* **2018**, *23*, 223–233. [CrossRef]
51. Huang, Y.R.; Dong, L. Characterization of pore microstructure and methane adsorption of organic-rich black shales in northwestern Hunan, South China. *Energy Explor. Exploit.* **2019**, *38*, 473–493. [CrossRef]
52. Xiao, Z.H.; Liu, J.S. Geologic characterization of a lower Cambrian marine shale: Implications for shale gas potential in northwestern Hunan, South China. *Interpretation* **2018**, *6*, T635–T647. [CrossRef]
53. Xiao, Z.H.; Tan, J.Q. Natural gas potential of Carboniferous and Permian transitional shales in central Hunan, South China. *J. Nat. Gas Sci. Eng.* **2018**, *55*, 520–533. [CrossRef]
54. Sun, Z.F.; Bai, Q.L. Quantitative evaluation of morphological characteristics of thin sand body: Taking the deltaic distributary channel sand body as an example in Shengtuo oil field of Dongying sag, east of Bohai Bay Basin. *J. Pet. Sci. Eng.* **2021**, *205*, 108749. [CrossRef]
55. Xu, X.; Feng, Q.H. Sedimentary characteristics and reservoir origin of the mound and shoal microfacies of the $Ma5_{1+2}$ submember of the Majiagou Formation in the Jingbian area. *J. Pet. Sci. Eng.* **2021**, *196*, 108041. [CrossRef]
56. Zheng, S.Q.; Yang, M. Controlling factors of remaining oil distribution after water flooding and enhanced oil recovery methods for fracture-cavity carbonate reservoirs in Tahe Oilfield. *Pet. Explor. Dev.* **2019**, *46*, 786–795. [CrossRef]
57. Yu, H.M.; Wang, Y.Q. Remaining oil distribution characteristics in an oil reservoir with ultra-high water-cut. *Energy Geosci.* **2022**. [CrossRef]

58. Zhang, Y.; Shi, Z. The influence of water level changes on sand bodies at river-dominated delta fronts: The Gubei Sag, Bohai Bay Basin. *Pet. Sci.* **2022**, *19*, 58–73. [CrossRef]
59. Ma, L.C.; Song, M.S. Exploration progress of the Paleogene in Jiyang Depression, Bohai Bay Basin. *Energy Geosci.* **2023**, *4*, 42–50. [CrossRef]
60. Guo, W.; Xu, G.Q. Influence of sediment supply rate on sequence stratigraphic architecture change: A case study from the Kaiping Sag, northern South China Sea. *Mar. Pet. Geol.* **2021**, *129*, 105106. [CrossRef]
61. Khalifa, M.K.; Mills, K.J. Predicting sequence stratigraphic architecture and its implication for hydrocarbon reservoir potential of the uppermost Silurian through Lower Devonian Winduck Interval, central Darling Basin of western New South Wales, SE Australia. *Mar. Pet. Geol.* **2022**, *142*, 105725. [CrossRef]